Journal of South American Earth Sciences 63 (2015) 360–374

Contents lists available at ScienceDirect

Journal of South American Earth Sciences

journal homepage: www.elsevier.com/locate/jsames

Inverse steptoes in Las Bombas volcano, as an evidence of explosive volcanism in a solidified lava flow field. Southern Mendoza-Argentina

Corina Risso [a, *], Claudia Prezzi [b], María Julia Orgeira [b], Francisco Nullo [c], Liliana Margonari [a], Karoly Németh [d]

[a] Departamento de Geología-IGEBA-Facultad de Ciencias Exactas y Naturales, Universidad de Buenos Aires – Intendente Güiraldes 2160 – Ciudad Universitaria, Pabellón II, Buenos Aires, C1428EG, Argentina
[b] Departamento de Geología-IGEBA-FCEN-UBA-CONICET, Argentina
[c] Newphoenix SRL., Argentina
[d] Massey University, CS-IAE, Volcanic Risk Solutions, New Zealand

ARTICLE INFO

Article history:
Received 7 October 2014
Received in revised form
28 July 2015
Accepted 14 August 2015
Available online 17 August 2015

Keywords:
Steptoes
Kipuka
Scoria cones
Lava field
Phreatomagmatism
Magnetic anomalies

ABSTRACT

Here we describe the unusual genesis of steptoes in Las Bombas volcano- Llancanelo Volcanic Field (LVF) (Pliocene – Quaternary), Mendoza, Argentina. Typically, a steptoe forms when a lava flow envelops a hill, creating a well-defined stratigraphic relationship between the older hill and the younger lava flow.

In the Llancanelo Volcanic Field, we find steptoes formed with an apparent normal stratigraphic relationship but an inverse age-relationship. Eroded remnants of scoria cones occur in "circular depressions" in the lava field. To express the inverse age-relationship between flow fields and depression-filled cones here we define this landforms as *inverse steptoes*.

Magnetometric analysis supports this inverse age relationship, indicating reverse dipolar magnetic anomalies in the lava field and normal dipolar magnetization in the scoria cones (e.g. La Bombas). Negative Bouguer anomalies calculated for Las Bombas further support the interpretation that the scoria cones formed by secondary fracturing on already solidified basaltic lava flows.

Advanced erosion and mass movements in the inner edge of the depressions created a perfectly excavated circular depression enhancing the "crater-like" architecture of the preserved landforms.

Given the unusual genesis of the steptoes in LVF, we prefer the term *inverse steptoe* for these landforms. The term steptoe is a geomorphological name that has genetic implications, indicating an older hill and a younger lava flow. Here the relationship is reversed.

1. Introduction

Volcanism in the Andean region is attributed to the subduction of the oceanic Nazca plate below the South American plate (Isacks et al., 1982) (Fig. 1A).

The Nazca plate subducts to the east under the Southern Volcanic Zone with an angle of c. 30° and with seismicity at average depths of 90–100 km under the volcanic arc (Yañez et al., 2002). The volcanic arc along the Andes comprises closely-spaced volcanoes that are still active (e.g: Calbuco volcano 2015; Cordón Caulle volcano 2011–2012; Chaitén volcano 2008, etc.).

Behind the active Andean volcanic arc the volcanic development of the 60,000 km^2 Payenia back-arc province has been suggested to be linked to the differential movements of the subducting Nazca plate and the overriding South American plate (e.g. Muñoz et al., 1989; Kay et al., 2006; Mazzarini et al., 2008; Folguera et al., 2009; Ramos and Folguera, 2011; Gudnason et al., 2012).

The name Payenia volcanic province, given to the area by Polanski (1954), has been used in more recent papers (e.g. Germa et al., 2010; Ramos and Kay, 2006. Gudnason et al., 2012; Quidelleur et al., 2009; etc.) and it can be divided from south to north in Rio Colorado Volcanic Field, Payún Matrú Volcanic Field, Nevado Volcanic Field, Llancanelo Volcanic Field and Northern segment (Gudnason et al., 2012; Folguera et al., 2009) or Diamante Volcanic Field (Morales Volosín, 2015).

The activity in the area is represented by large composite volcanoes such as Payún Matrú, Payún Liso and Cerro Nevado that have produced evolved volcanic material including the large

* Corresponding author.
E-mail address: corina@gl.fcen.uba.ar (C. Risso).

http://dx.doi.org/10.1016/j.jsames.2015.08.007
0895-9811/

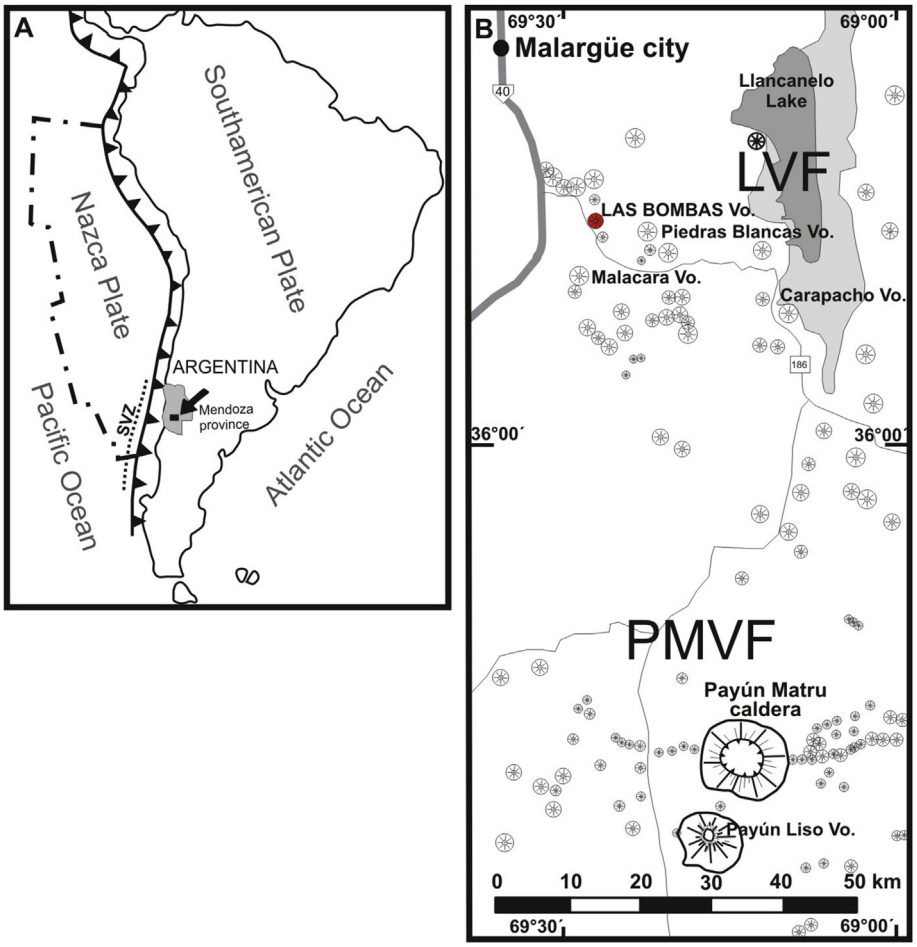

Fig. 1. A: Location map of South America and Argentina, highlighting the Southern Volcanic Zone (SVZ) and the subduction of the Nazca plate beneath the South American plate. B: Map of Llancanelo Volcanic Field (LVF) and Payún Matru Volcanic Field (PMVF) with location of Las Bombas Volcano.

caldera forming eruptions of Payún Matrú (Llambías, 1966; Bermúdez, 1988; Ramos and Kay, 2006; Folguera et al., 2009; Germa et al., 2010). Surrounding the larger volcanoes there are two volcanic fields represented by monogenetic scoria cones of almost exclusively basaltic composition often aligned and concentrated in small clusters: the Llancanelo and Payún Matrú Volcanic Fields (Fig. 1A and B).

Volcanism in Payenia encompasses activity from the Pliocene (Kay et al., 2006; Lambías et al., 2010; Gudnason et al., 2012) to the youngest activity within the Payún Matrú caldera (Escorial del Matrú), dated at 7 ± 1 ka (Germa et al., 2010).

The Llancanelo Volcanic Field (LVF), (Figs. 1B, 2A and 5E) covers an area of 10,700 km^2 in the south-eastern region of the province of Mendoza, Argentina, between latitudes 35° 39′ and 35° 50′ S and longitudes 69° and 69°30′ W, approximately 200 km east of the trench in the Southern Volcanic Zone (Fig. 1A).

In addition, south of the LVF, the Payún Matrú Volcanic Field (PMVF) surrounds the Payún Matrú shield volcano (Fig. 1B). The Payún Matrú shield is a complex volcano with an 8 × 6.5 km wide summit caldera, with trachybasalts (hawaiites) to trachytes lava flows, domes, coulees and extensive pyroclastic flow deposits (Hernando et al., 2014; Hernando et al., 2012; Llambías, 1966; González Díaz, 1972; Ramos and Key, 2006). $^{40}Ar/^{39}Ar$ radiometric dating shows that the Payún Matrú volcano has been active since at least 700.6 ± 10.6 ka (Hernando et al., 2014) and should be considered an active but dormant volcano. The youngest activity within the caldera has been dated at 7 ± 1 ka (Germa et al., 2010).

Volcanic activity in the LVF (Fig. 1B) was primarily of Hawaiian and Strombolian type, resulting in at least 150 scoria and/or lava spatter cones with edifice heights ranging from 50 to 150 m, crater diameters ranging between 150 and 200 m, and slope angles varying between 16 and 27° (Inbar and Risso, 2001). Preserved pyroclastic deposits of the scoria and spatter cones are typically coarse ash and lapilli that consist of red, scoriaceous pyroclasts with common meter-sized ballistic bombs and blocks of vesicular and degassed spindle-shaped pyroclasts. Both, large vesicular, spindle-shaped lava bombs and blocks as well as bread crusted bombs and blocks with a diameter up to 3.5 m, are common.

In well-drained areas with large volumes of near-surface and/or ground water, tuff rings and/or maar volcanoes form (Martin and Németh, 2004). The presence of subordinate phreatomagmatic volcanoes in a volcanic field could indicate variations in hydrogeology of the volcanic field, or variations of the water saturation state of the sub-surface sediments or rock units over time (Aranda-Gomez and Luhr, 1996; Gutman, 2002). Such variations are also noted to take place during the total life span of a volcanic field resulting age-clustered volcanoes dominated by eruption styles related more to dry versus wet external eruptive environments (Kereszturi et al., 2011; Kereszturi and Németh, 2012).

The Las Bombas (LB) volcano is located in the low-lying regions

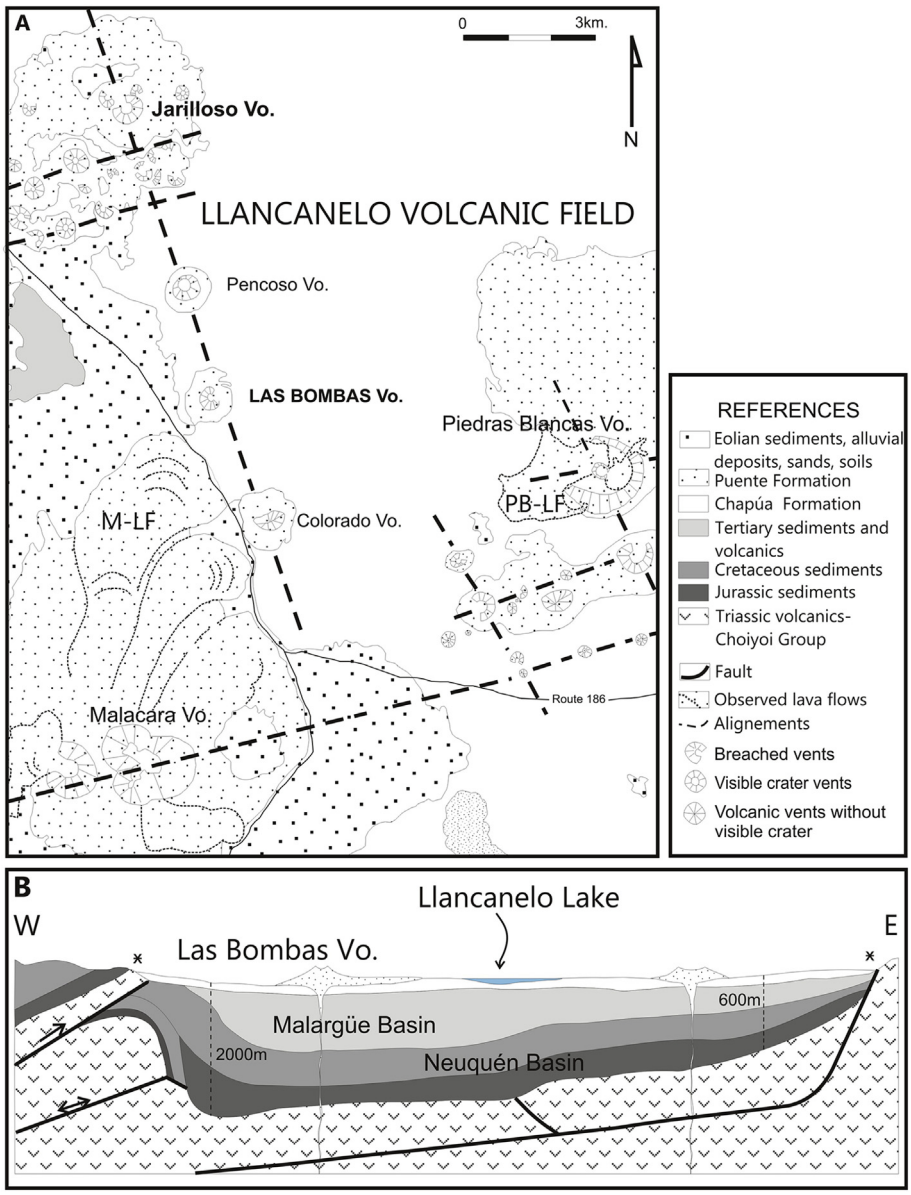

Fig. 2. A: Geological map of Las Bombas volcano and surroundings in the LVF. B: W–E profile of Malargue basin stratigraphic section (out of scale).

of the LVF near the saline and endorheic Llancanelo Lake (Figs. 1B and 2B). Besides the scoria cones in the LVF (more than 879 vents in LVF and PMVF, Mazzarini et al., 2008), at least 30 identified volcanoes show evidence of explosive eruptions involving varying degrees of magma–water interaction (Llambías et al., 2010). These are unusual in the context of the present and inferred syn-eruptive semi-arid climate of the eastern Andean ranges. The climatic and the physiographical conditions of the volcanic field are inferred to be similar to the present day ones, i.e., semi-arid conditions with strong westerly winds (Delpino, 1993). The region has today a temperate-arid North-Patagonian climate with an average annual temperature of 11.7 °C, an average minimum temperature of 4.4 °C and an average maximum temperature of 19.8 °C. Precipitation regime does not exceed 200 mm/year in the plains (Violante et al., 2010).

According to Delpino (1993) paleoclimatic-paleoenvironmental conditions were inferred based on analysis of fossils in the lacustrine sediments. Results indicate that the syneruptive conditions were shallow lacustrine surrounded by moderately vegetated scrublands. However, the proto-Llancanello lake is estimated to be larger and deeper than the modern lake, covering an area of 5000 km^2 with a depth 50 m larger than the present one.

Most of the volcanic structures in the proximity of the present day Llancanelo lake shoreline resulted from explosive phreato-magmatic eruptions, and they consist of tuff rings and tuff cones (Risso et al., 2008). Olivine basalt magma was involved in the water interaction. It is inferred that fluctuating water levels of Llancanelo Lake could have influenced the hydrogeology of the lake basin and hence the eruptive style of volcanism (Risso et al., 2008) or, on the other hand, that a structural control could favour the rise of water through fractures. Large water masses can influence the laterally interconnected ground water aquifers, especially those sandwiched between thick lava flows, as demonstrated in the case of the phreatomagmatism along the Western Snake River Plain in Idaho (Godchaux et al., 1992).

Here we focus on the northern Llancanelo Volcanic Field,

particularly in LB volcano (Figs. 1B, 4B and 5A and E). LB volcano is an eroded but still recognizable scoria cone located in a circular depression, suggesting that it was there when the lava flow field formed, and, therefore the lava flow engulfed it completely, like an island in a sea of lava. While this explanation seems reasonable, the common presence of similar landforms in this part of the field justified the need to establish correctly the stratigraphic relationship between lava flow fields and these circular features on it.

Lava often flows around hills or mountains, forming a volcanic morphology known as *steptoe*, or in the Hawaiian language *kipuka*. As defined, a steptoe is *"An isolated hill or mountain of older rock surrounded by a lava flow. Syn*: *dagala"* (Bates and Jackson, 1980). A clear example of *steptoe* is seen in Fig. 4A and C, with an older pyroclastic cone surrounded by a younger lava flow. These "islands" have been called *steptoes*, *dagalas* or *kipukas*. This landform is named after Steptoe Butte, a quartzite protrusion over 400 million years old, jutting out of the 15–7 million year old Columbia River Basalts near Colfax, Washington, U.S.A. (Easterbrook, 2003). The steptoe hill or mountain is assumed to be older than the surrounding lava flow.

In this paper, we explore these morphologies identified in southwest Mendoza province closely resembling *steptoes* with the difference that they have their central cones suspected to be younger than the surrounding lava flow fields and thus could be defined as *inverse steptoes*, (Fig. 4B), *i.e*. where the surrounding lava flow is older than the pyroclastic cone. With the aim of testing the timing of cone formation and lava flow field emplacement, as well as to understand the 3D architecture of these volcanoes-within-circular-features, geological mapping and geophysical studies were completed including detailed topographic, magnetic and gravimetric land surveys.

Perhaps detailed and well located radiometric analysis may answer this uncertainty, but here we try to use geological and geophysical data to explain this situation.

2. Geologic setting

High-density scoria cone fields are those containing large number of closely spaced scoria cones erupted over a relatively short period of time (e.g. large number of volcanoes per area). Such volcanic fields are common in intra-continental regions such as the San Francisco Volcanic Field, Arizona (Conway et al., 1997), Pali Aike, Argentina (Mazzarini and D'Orazio, 2003), or Al Haruj in Libya (Martin and Németh, 2006).

The eruption of extensive Pliocene to Recent back-arc lava fields in southeastern Mendoza province (LVF and PMVF, Fig. 1B) are interpreted to be linked to the melting of hydrated mantle after a transient episode of Neogene shallow subduction (Ramos and Kay, 2006). In Pliocene to Quaternary times, a return to steeper subduction, with more pronounced steepening to the north, ended the arc-like magmatism in the foreland far east of the trench (Ramos and Kay, 2006). This was followed by widespread Pliocene to Quaternary mafic volcanism with a progressively more intraplate-like chemical signature that is best explained by the steepening of the subducted slab (Kay, 2002; Ramos and Kay, 2006).

Vent density distribution is strongly conditioned by pre-existing crustal anisotropies (Hernando et al., 2014; Bermúdez et al., 1993). The overall E–W vent density distribution in PMVF is controlled by pre-existing crustal structures (Mazzarini et al., 2008; Llambías et al., 2010; Hernando et al., 2014). In the central zone of Payenia the volcanic eruptions formed NW–SE vent alignments, reaching up to 60 km in longitude (Bermúdez et al., 1993), and were related to reactivation of Paleozoic faults of the volcanic basement (Llambías et al., 2010). Eruptions in the LVF have NW–SE trending alignments, as shown in the alignment of vents both east and west of Llancanelo lake (Delpino, 1987; Ninci, 1993) (Figs. 1B and 5E).

The rocks of LVF are alkaline olivine basalts, with a silica content ranging between 46 and 52% and $Na_2O + K_2O$ ranging between 3.5 and 6% (Bermúdez et al., 1993). The homogeneous alkali-basalt composition of the back-arc lavas indicates a low degree of differentiation and relatively short travel time from deep mantle sources (Bermúdez and Delpino, 1989; Bermúdez et al., 1993). Volcanic activity started in the early Pliocene and probably continued until the last thousands of years, including the Chapúa, Puente and Tromen Formations (Nullo et al., 2005). The eruptive products of the youngest (Holocene) volcanism (Tromen Formation) is not represented in the LVF.

The back-arc basalts of the LVF are the uppermost basin-filling formations of a tectonic depression defined by the Tertiary Malargüe Basin (Fig. 2B). The basin is characterized by differentially elevated basement blocks of Permotriassic mesosillicic and acid volcanics. The basement, structure, and different sedimentary units filling the Tertiary Malargüe and the Mesozoic Neuquén Basins are shown in Fig. 2B. The eastern and western limits of the Malargüe Basin are defined by NW-SE-trending fault lines (see * in Fig. 2B). The western fault is more or less parallel to the ±153° trending volcano alignment formed by the Jarilloso, Pencoso, Las Bombas, and Colorado volcanoes (Fig. 2A). The eastern fault is parallel to the eastern margin of the present-day shoreline of Llancanelo Lake (Figs. 1B and 2B). The uppermost basin filling formations, unconformable with the underlying units, are the back-arc basalts grouped into the older Chapúa Formation and the younger Puente Formation (Nullo et al., 2005).

Basalts of Chapúa Formation (Nullo et al., 2005), are of a glossy black colour, with texture that goes from vesicular at the top to dense, non-vesicular at its base. Extensive, fresh-looking lava flows are predominantly *pahoehoe* type, with tumuli, ropy lava and occasional lava tubes and skylights (Bermúdez y Delpino, 1989; Németh et al., 2008), and subordinate *aa* type. The source of these extensive lava flows is unknown due to the lack of a mappable relationship between lava flows and volcanic edifices as a result of advanced erosion. Chapúa Formation has been generated by successive overlapping (37–40 m thick) lava flow units and forms the depositional and palaeo surface upon which most of the new and younger volcanoes (such as Las Bombas, Pencoso, Colorado, etc. in Figs. 2A and 5 A–E) formed.

Overlying the previous rock units is the Puente Formation (Nullo et al., 2005), which also consists of extensive lava flows related to volcanic cones that are still recognizable. The Puente Formation basalts are well-exposed in Malacara's lava flow (Fig. 2A, M-LF) and in Piedras Blancas' final lava flow (Fig. 2A, PB-LF).

Las Bombas volcano is formed on a basaltic plateau of the oldest Chapúa Formation. Its pyroclastic products belong to the younger Puente Formation. Chapúa and Puente olivine basalts are similar, differing only in size of phenocrysts and groundmass. Basalts of Chapúa Formation have 30% phenocrysts (Bermúdez et al., 1993; Risso et al., 2008), and olivine phenocrysts reach 6 mm (Figs. 3A and 6D). The rock textures of Puente Formation basalts are quasi aphiric, with 1–5% phenocrysts (Figs. 3B and 7A, C and D) (Bermúdez et al., 1993; Risso et al., 2008), with considerable amounts of coarse euhedral olivine crystals (1–3 mm) in a pilotaxic-subophitic, sometimes intersertal, groundmass of plagioclase and titanoaugite, epidote and pale-brown sideromelane glass.

New radiometric and cosmogenic ages can partially help to understand the sequence of volcanic events west of Llancanelo lake.

The sample dated by Gudnason et al. (2012) from Cerro Jarilloso, is 0.16 ± 0.07 Ma (^{40}Ar- ^{39}Ar) and would be representative in age for much of the latest volcanic activity in the area. This is confirmed by

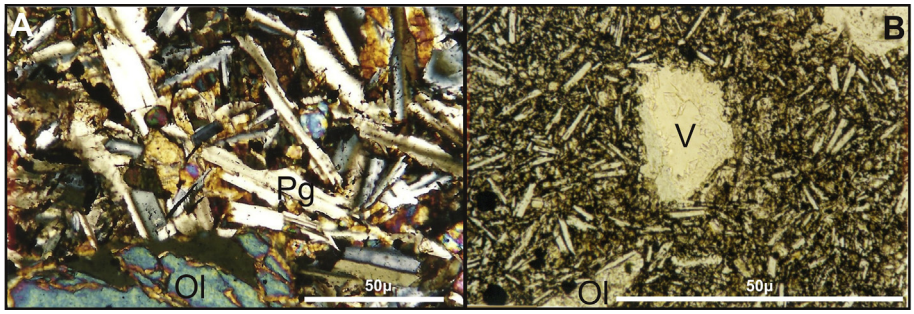

Fig. 3. A: Photocmicrograph in plane polarized light showing greater pilotaxic texture with larger olivine (Ol) and plagioclase (Pg) phenochrysts of Chapúa rocks. B: Photocmicrograph in transmitted light showing pilotaxic texture cuasi aphiric with vesicles (V) partially filled with zeolites and olivine (Ol) microphenochrysts in basalt rocks of Puente Formation.

the ^{40}Ar- ^{39}Ar ages of Espanon (2010) of 0.12 ± 0.13 Ma and 0.40 ± 0.07 Ma for the dated Llancanelo lavas sampled west of the Llancanelo lake. However, location of sampled sites is not completely accurate.

Cosmogenic surface exposure ages were obtained from sample LL3 (tumulus in pahoehoe lava, 1.5 km southwest of LBV, 73,7 ± 1.1 ka ^{3}He and 49.7 ± 2.2 ka ^{21}Ne) (Espanon et al., 2014).

Taking into account that ages determined by different methods (cosmogenic and radiometric) cannot be directly compared, we decided to consider the more traditionally used Ar/Ar data.

Risso et al. (2008) related Cerro Jarilloso and Las Bombas volcano to a single volcanic event occurred along the same lineament (Fig 2). Thus, we assign an approximate age of 0.16 Ma to the volcanic activity of Las Bombas. The surrounding lavas could have an age comparable to the 0.40 Ma age reported by Espanon (2010) and assigned by Gudnason et al. (2012) to the Llancanelo lavas sampled west of the Lake Llancanelo. If these correlations are adequate, they support our model of a younger volcano surrounded by older lavas.

3. Scoria cones of the LVF

Scoria cones are the most common manifestation of subaerial small-volume, short-lived volcanism on Earth and are generally considered to be a result of mild explosive eruption of mafic magmas in a short period (weeks to months), (Vespermann and

Fig. 4. A: Steptoe or Kipuka in the PMVF. Older cinder cones (white arrow) surrounded by "aa" younger lava flow. B: Las Bombas volcano surrounded by pahoehoe lava flows in LVF. In this case the volcano is younger than the environs lava flows C: Image from Google Earth shows a scoria cone 17 km NE of Paricutín volcano in the Trans-Mexican Volcanic Belt. Older scoria cone covered by pine forests surrounded by younger lava flows with scarce vegetation. See the depression around the cone similar as in Las Bombas volcano, but different in age. In these case the depression is due to degradation of the cone (Hasenaka and Carmichael, 1985).

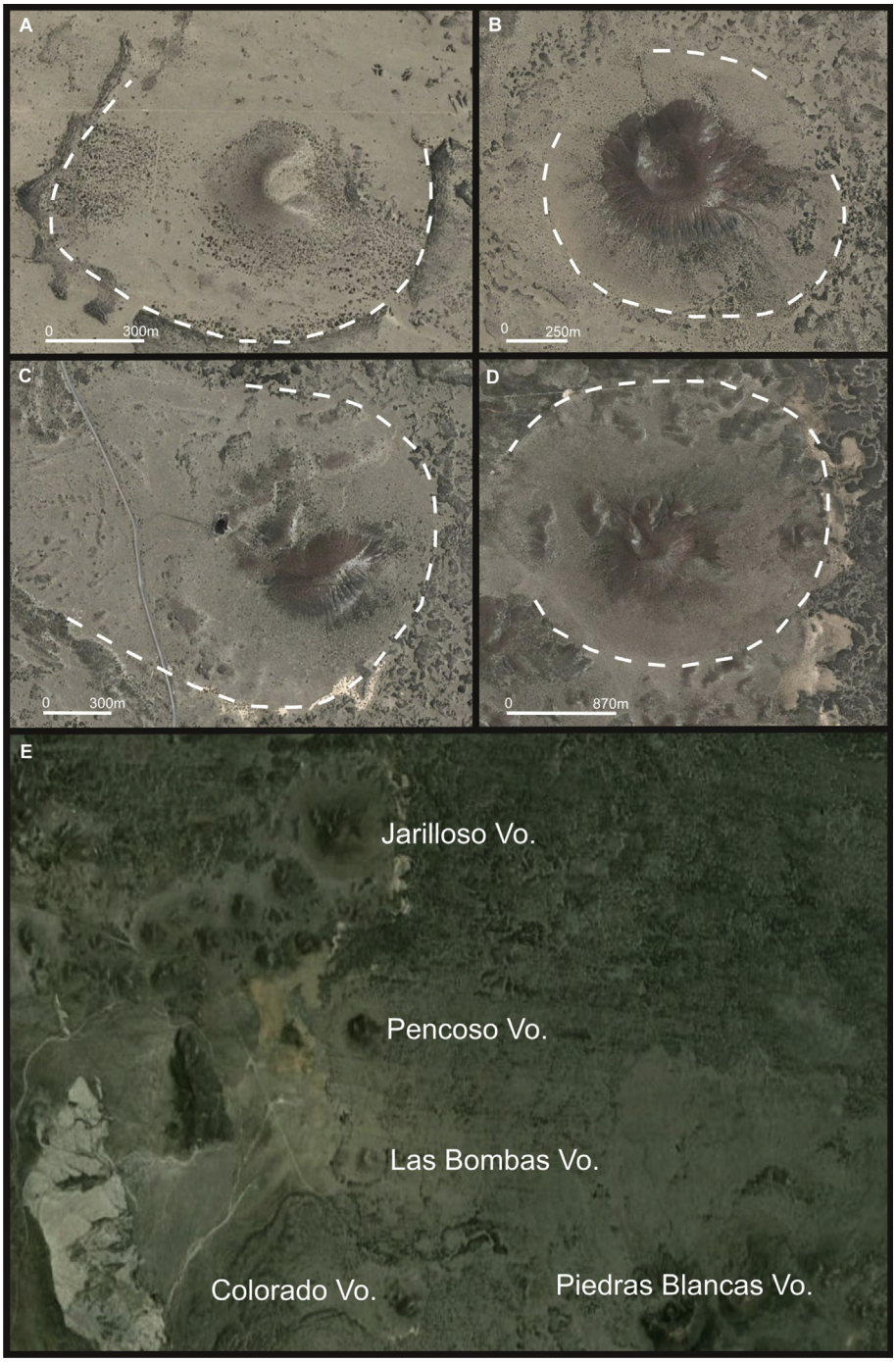

Fig. 5. A: Las Bombas Volcano. B: Pencoso Volcano. C: Colorado Volcano D: Jarilloso Volcano. E: General view of Las Bombas, Pencoso, Colorado and Jarilloso volcanoes with "circular pattern" (dotted white line) in the LVF. LVF comprise the entiere image, excluding the southwest side with outcrops of white Cretaceous limestones and darker Miocene andesites. Images from Google Earth.

Schmincke, 2000). Scoria cones are commonly formed from relatively simple eruptions, but there is evidence of exceptionally long-lived cinder cone activity such as the Paricutin volcano in Mexico (Foshag and Gonzalez, 1956). In spite of the long eruption duration, scoria cones are generally defined as monogenetic volcanoes (Kereszturi and Németh, 2012). Monogenetic traditionally refers to volcanoes that erupt only once during their eruptive history (Walker, 1993; Valentine and Gregg, 2008; Németh, 2010).

The volcanic cones of the LVF are predominatly scoria cones and subordinate tuff rings and tuff cones. The scoria cones studied are located in a volcano alignment formed by the Jarilloso, Pencoso, Las Bombas, and Colorado volcanoes (Fig. 2A); Las Bombas (LB) is the most representative of this group.

The measured morphometric parameters of scoria cones are given in Table 1.

Jarilloso, Pencoso, Las Bombas, and Colorado volcano are small-volume (<0.027 km^3) scoria cones, following the equation of a truncated cone used in Dóniz-Páez et al. (2008). Their height-width ratio is about 1:5 to 1:16 and is compatible with scoria cones documented by Heiken (1971) and Dóniz-Páez et al. (2012).

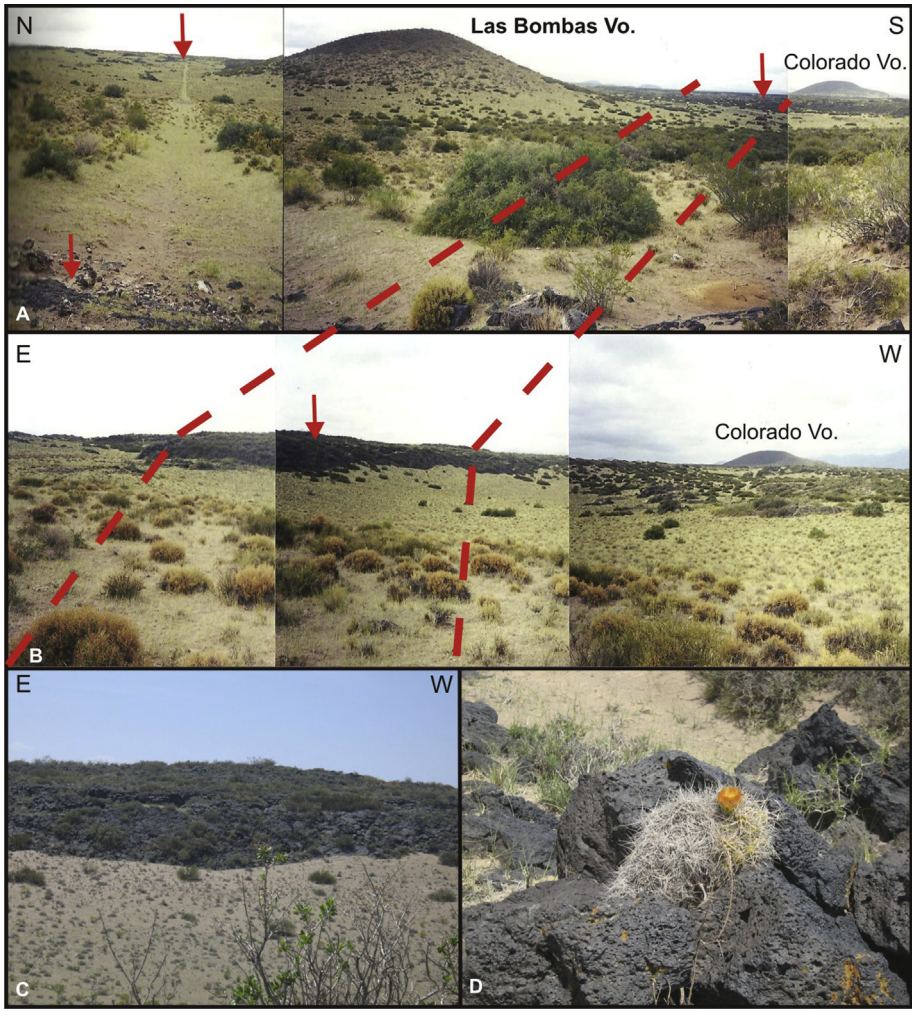

Fig. 6. A: Las Bombas volcano in the center, surrounded by a slight depression and the "older lavas" at the far end (red arrows). Red arrows mark the edge of the Chapúa Fm. around the cone. Dotted red line shows part of the "older lavas" front at bottom in Fig. 6A and on foreground in Fig. 6B. B: Shrubs and sands cover the "circular depression" around Las Bombas cone. C: Front view of the "oldest lava" flows and shrubs-sands of the circular depression around the cone. D: detail of the black vesiculated pahoehoe lavas surrounding the volcano. Cactus as scale. (For interpretation of the references to colour in this figure legend, the reader is referred to the web version of this article.)

The scoria cones are approximately circular in map view, and few are breached (e.g. a not entire well-defined crater rim) toward N and NE. They have small central bowl-shaped craters, excluding the Colorado volcano which is more eroded than the others and without an identifiable crater (Fig. 5C). The cones in the LVF are moderately preserved with well-developed rills and sands covering the gentle slopes. Slope angle values are less than 20° (Table 1) (as measured by a combination of topographic cross sections, oriented field photography and spot elevation measurements applying trigonometric consideration). The cones are composed of coarse-grained red scoriaceous lapilli, blocks and bombs.

The textural characteristics of the pyroclasts of scoria cones, such as their high vesicularity, fluidal shape, and their dark, often red colour, indicate a magmatic degassing and fragmentation history due to explosive eruptions (Vergniolle et al., 1996; Vergniolle and Brandeis, 1996; Vergniolle and Manga, 2000; Jaupart and Vergniolle, 1988), commonly referred to as Strombolian-style explosive eruptions.

The usual intercalation of scoria beds in the studied scoria cones of the LVF, with welded fall deposits and/or clastogenic lava flows, indicates a sudden and common change in eruption style from Strombolian to Hawaiian and vice versa (Valentine and Gregg, 2008; Sumner, 1998) reflecting variable volcanic conduit dynamics in the course of the eruption. Lava spatter near the vent, typically along the crater rim of the studied cones form strongly welded, agglutinated, red, slightly bedded sequences with large spindle or highly vesicular fluidal shaped bombs.

4. Phreatomagmatic volcanoes of the LVF

While the volcanic cones of the LVF are predominantly scoria cones, some have been identified as products of phreatomagmatic eruptive phases as inferred by their pyroclastic products (Risso et al., 2008). Volcanoes with some thin basal or inter-bedded pyroclastic units that indicate explosive phreatomagmatic phases or a complete pyroclastic succession typical for tuff rings and tuff cones primarily formed are located in the northwest and northeast low-lying regions of the LVF nearby the present day Llancanelo Lake such as Malacara, Piedras Blancas and Carapacho volcanoes (Figs. 1B and 2A). To date, no phreatomagmatic volcanoes have been identified in the PMVF.

To distinguish the pyroclastic units formed due to phreatomagmatic explosive eruptions from pure magmatic fragmentation-driven explosive eruptions in the LVF, a characteristic colour difference, grain size distribution difference, and bedforms typical for pyroclastic density current transportation and deposition were

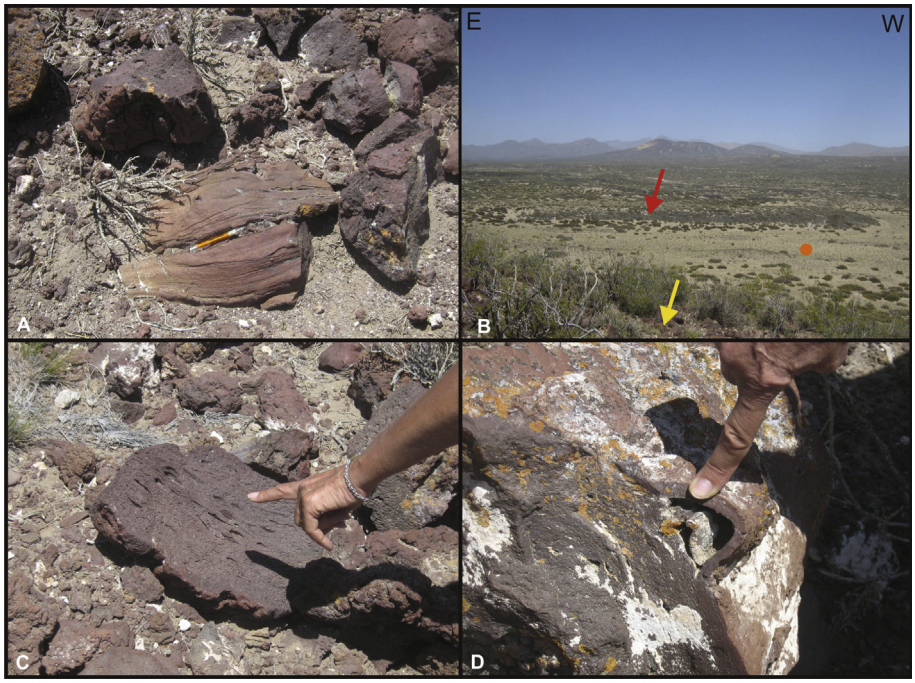

Fig. 7. Reddish basalts of Puente Formation. A: basalt blocks and red spindle bombs. B: Photo taken from the top of Las Bombas volcano to the South. In foreground there are red blocks and bombs (yellow arrow). It in half, the volcano is located in a slight circular depression (orange dot) filled with sand and grass. In the background (red arrow) the 3 m shoulder of "older lavas". C: Blocks and bombs with lower crystallinity and large and elongated vesiculation. D: skin of congealed lava formed on the exterior of the bombs during the molten state. (For interpretation of the references to colour in this figure legend, the reader is referred to the web version of this article.)

Table 1
Cone parameters. Cone height: H_{co}, basal width of cone: W_{co}, crater diameter: W_{cr}, slope angle: α, cone volume: V_{co}.

Volcano	H_{co}	W_{co}(m)	W_{cr}(m)	α (°)	V_{co}($km^{3)}$	H_{co}/W_{co}
Colorado	33	520	–	16	–	0.06 = 1:16
Las Bombas	50	330	129	23	0,0085	0.15 = 1:6
Pencoso	53	552	235	19	0,0274	0.09 = 1:11
Jarilloso	97	1059	240	20	0,0284	0.09 = 1:11

used. In addition, the morphometry of the volcanoes were also used to distinguish volcanoes formed due to magmatic versus phreato-magmatic explosive eruptions. Volcanoes with wide craters and low slope angles (normally less than 15°) with matrix-rich tuff and lapilli tuff sequences were inferred to be tuff rings such as the Piedras Blancas volcano (Figs. 2A and 5E).

The Piedras Blancas volcano (Figs. 1B and 2A) is a 140 m-high tuff ring measured from its base to its crater rim crest. The tuff ring crater is 1150 m in diameter, with a circular shape breached to the W-NW (Fig. 2A) and a small breached nested scoria cone inside it. Its latest volcanic activity produced massive bluish *aa* lava flows (Fig. 2A see PB-LF) with rubbly levee-margins in the SW side of the vent. These lava flows reached a distance of up to 2 km NW from their source. The main pyroclastic cone consists of a 90 m-thick, monotonous, yellowish-grey scoriaceous pyroclastic fall and surge deposit. Beds dip outward radially away from the vent at 24–28° (Risso et al., 2008).

5. Las Bombas volcano

Scoria cones, like Las Bombas, (LB) volcano (Figs. 1B, 2A and 5A), are by far the most common type of volcanoes in the LVF. LB is a small pyroclastic cone that is no more than 50 m in height (Fig. 6A) and covered by sand, grass and small bushes. It has a breached crater towards the east. Rills and gullies are not well-developed and white aeolian siliciclastic sand and acidic volcanic ash from the 1932 A.D. Quizapu eruption cover its gentle slopes. The cone base to crater diameter ratio (H_{co}/W_{co}) is 0.15 (Table 1), consistent with a ratio expected for scoria cones (Dóniz-Páez et al., 2012; Fornaciai et al., 2012; Gilichinsky et al., 2010; Inbar et al., 2011; Kereszturi et al., 2013; Kereszturi et al., 2012; Kervyn et al., 2012).

Although the volcano is covered by sand and shrubs, scattered banded basalt blocks (13–40 cm diameter) and reddish bombs have been observed from the middle slope to the top of the cone (Fig. 7B, yellow arrow). Blocks and bombs have lower crystallinity and large (eg: 3 × 0.8 cm) and oriented vesicles (Fig. 7C).

At the eastern flank, and typically along the crater rim of the cone, there are many agglutinated bombs and spindle-shaped fluidal bombs (Fig. 7A). Some of these reddish bombs have a thin skin of quenched lava indicating they were molten state upon landing on the depositional surface (Fig. 7D). Bombs and blocks from the top of LB volcano are solidified lava spatters that landed on the surface in a molten state allowing agglutination of the spatter, suggesting periods of high eruption rates. These observations are consistent with a Hawaiian-style eruption.

LB is located in a slight circular depression filled with sand and grass (Fig. 7B, orange dot), as are the Pencoso, the Colorado and the Jarilloso volcanoes (Fig. 5A–E). The depression averages 1.13 km in diameter at the LB volcano (Figs. 5A and 8A and B). A detailed map of the LB volcano and its surroundings remarking the distribution of older lavas and the pattern of the circular depression and ledge around the cone is shown on Fig. 8A. Fig. 8B is a sideway view of the depression, showing in the foreground the slope of LB volcano, the depression around the volcano (Fig. 5A), and in the background the 3 m shoulder of older lavas (Fig. 7B, red arrow). All contacts are covered by vegetation or buried by sand (Fig. 6B and C). A ledge is especially well-preserved in the southern sector of the LB volcano, in Pencoso and Jarilloso volcanoes and to the SE in the Colorado volcano (Fig. 5, B–E). Such circular depression has also been found in other volcanoes of LVF such as around the Pencoso cone (1.19 km

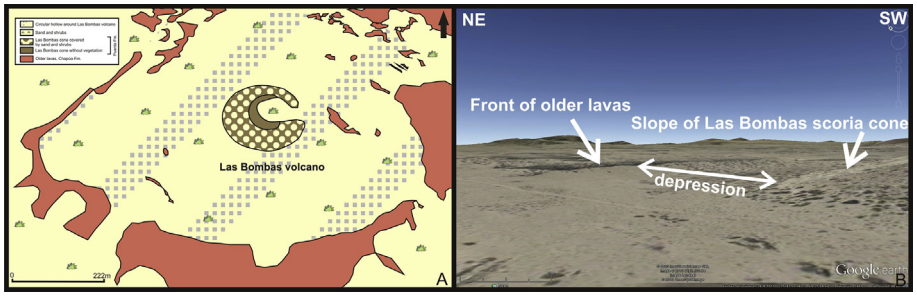

Fig. 8. A: Detailed map of Las Bombas volcano and its surroundings remarking the distribution of "older" lavas and the pattern of the circular depression and ledge around the cone. B: is an sideway view of the depression, showing in the foreground the slope of Las Bombas volcano, secondly the depression around the cone and the shoulder of black Chapúa basalts. Image of Google Earth.

in diameter, Fig. 5B), Colorado volcano (1.37 km in diameter, Fig. 5C) and Jarilloso cone (2.31 km in diameter, Fig. 5D).

As described previously, the Chapúa basalts, the "older basalts", are black (Fig. 6C and D), extensive (Fig. 2A) and are predominantly of *pahoehoe* type in the LVF, with tumuli, ropy lava and occasional lava tubes and skylights. Chapúa's basalts have 30% large olivine phenocrysts (6 mm) (Fig. 3A). In contrast, the Puente basalts ("the younger") are quasi aphiric, with 1–5% phenocrysts of euhedral olivine crystals (1–3 mm) and forms predominantly *aa* lava flows (Fig.s. 7A–D and 3B). The above outlined petrographic difference between the older Chapúa and younger Puente basalts allow us to easily distinguish one type of basalts from the other and use this textural information as a field tool to establish stratigraphic relationships between lava fields hosting the circular depressions and coherent lava bodies associated with cones filling the same depressions Fig. 6D (Chapúa) from Fig. 7 A, B and C (Puente).

These "circular landforms" around the scoria cones caught our attention because they seemed to be very common lava fields features in other localities such as those reported from the Quaternary Trans-Mexican Volcanic Belt, (see Fig. 4C) where younger lava flows surround older cinder cones. The problem is that the locations reported here differ from those described elsewhere by having a reverse stratigraphic relationship between the cones and the lava fields hosting the "circular depression". Based on the rock textural data, the depressions documented here are hosting a younger cone and best described as an *inverse steptoe*.

6. Geophysical studies

In order to geophysically characterize the study area and test the genetic relationship and stratigraphic order between extensive lava fields surrounding the volcanoes, geophysical methods were employed to describe the detailed topographic architecture (Fig. 9), the magnetic and gravimetric signatures of the LB volcano and its relationship with the flow field-building lavas. Also paleomagnetic studies (Fig. 10) were carried out in order to infer the chronologic order of the genetic processes. If the central cones were younger than the surrounding lava flow field, samples obtained from such surrounding lava flow should have registered random directions of the characteristic remanent magnetizations (ChRMs) due to the fracturing and the consequent scattering of the resulting blocks. On the contrary, if the central cones were older than the surrounding lava flow field, directions of the characteristic remanent magnetizations registered by samples collected from such surrounding lava flow field should be parallel after tilt correction. The applied methodology is described in detail in appendix 1.

The magnetic survey shows two dipolar magnetic anomalies (Fig. 11). One of them corresponds to the basaltic pahoehoe flows forming the border of the circular pattern associated with LB volcano. This dipolar anomaly presents a minimum ~of −200 nT to the north of the profile and a maximum ~ of 1900 nT to the south (Fig. 11, black arrows). Ten oriented hand samples from this basaltic flow were taken for natural remnant magnetization (NRM) intensity measurements in the laboratory, using a SQUID 2G SSR cryogenic magnetometer. The intensity of the NRM has an average value of 11,378 mA/m. This intensity of the NRM would control one of the detected dipolar magnetic anomalies, which is of reverse character. Such magnetic signature indicates that these basalts cooled during a period in which the polarity of the geomagnetic field was opposite to the present one. The other dipolar magnetic anomaly, located in the centre of the profile, is closely associated with the scoria cone (Fig. 11). It presents a maximum ~ of 1700 nT to the north of the profile and a minimum ~ of −100 nT to the south (Fig. 11, red arrows), being of normal polarity. This anomaly would suggest that the formation of the scoria cone occurred during a period in which the polarity of the geomagnetic field was like the present one.

The complete Bouguer anomaly presents a minimum value ~ of −5 mGal, which correlates perfectly with the maximum height of the scoria cone (~50 m) (Fig. 11). This negative anomaly indicates the existence of a mass deficit below the cone. All the rocks described in the area correspond to basaltic flows. Although textural differences or different lithofacies (of the same composition) (i.e. spatter vs coherent lavas) could exist, the corresponding density contrast would not be enough as to produce the detected complete Bouguer anomaly. Therefore, the negative anomaly could be satisfactorily explained by means of the existence of secondary fractures below the cone generated during the volcanic eruption.

As was previously mentioned, if the central cones were younger than the surrounding lava flow field, the ChRMs should have registered random directions due to hydrothermal activity, high temperatures, fracturing and the consequent scattering of the resulting blocks, etc. On the other hand, if the central cones were older than the surrounding lava flow field, directions of ChRMs should be parallel after tilt correction. Isolated ChRMs have positive and negative inclinations, and show a noticeable dispersion. Consequently, the fold test (McFadden, 1990) is indeterminate. However, the tilt corrected final mean direction presents a larger confidence interval than the uncorrected one. This fact would indicate that the central cones are younger than the surrounding lava flow field.

Our results suggest that the volcanic processes in the area took place in two separate events during distinct time spans. The oldest one occurred during a period in which the polarity of the geomagnetic field was opposite to the present one. The reversely magnetized basaltic flows, which form the border of the studied circular depression, were assigned to Chapúa Formation (see Introduction and Geologic Setting). Considering these facts and the

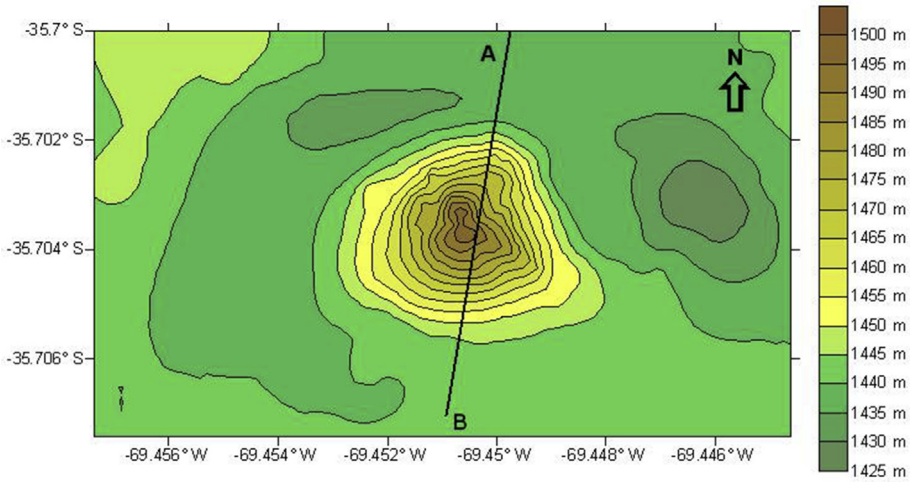

Fig. 9. Detailed topography surveyed in the field of Las Bombas volcano and its surrounding "circular pattern". The location of the magnetic and gravity profile presented in Fig. 11 is also shown (AB).

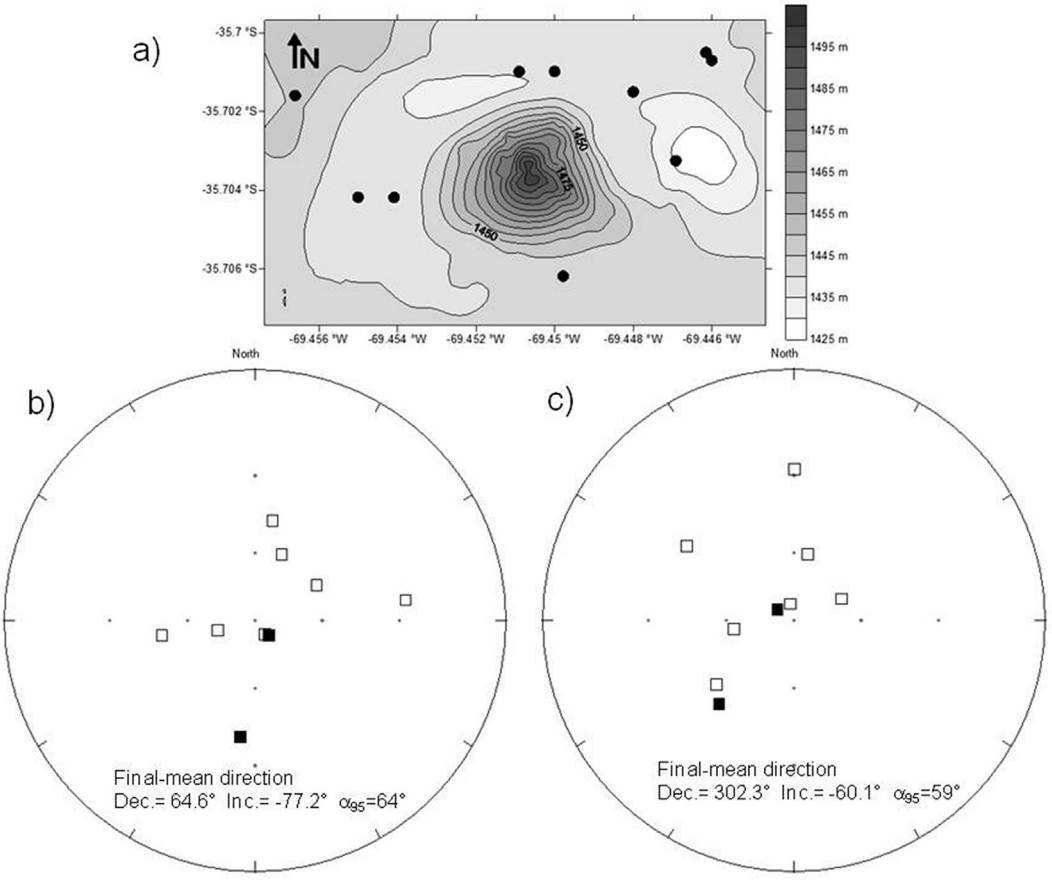

Fig. 10. Map showing location of collected hand samples. b) Equal angle stereoplot showing tilt corrected ChRMs directions. c) Equal angle stereoplot showing ChRMs directions without tilt correction. Open symbols: negative inclination, Black symbols: positive inclination.

age model proposed in this contribution, such basaltic flows could have solidified during the reverse subchron Bermuda in the chron Brunhes (around 0.4 Ma, Chanell et al., 2012) (e.g. Lanza and Meloni, 2006). On the other hand, according to the geological observations (see Introduction and Geologic Setting), the youngest volcanic event associated with the formation of the scoria cone, responsible for the normal dipolar magnetic anomaly detected, should have occurred during the normal polarity of the Bruhnes chron (<0.7 Ma).

7. Results and discussion

Consequently, the results of the geological and geophysical studies carried out here suggest that the scoria cone located in the

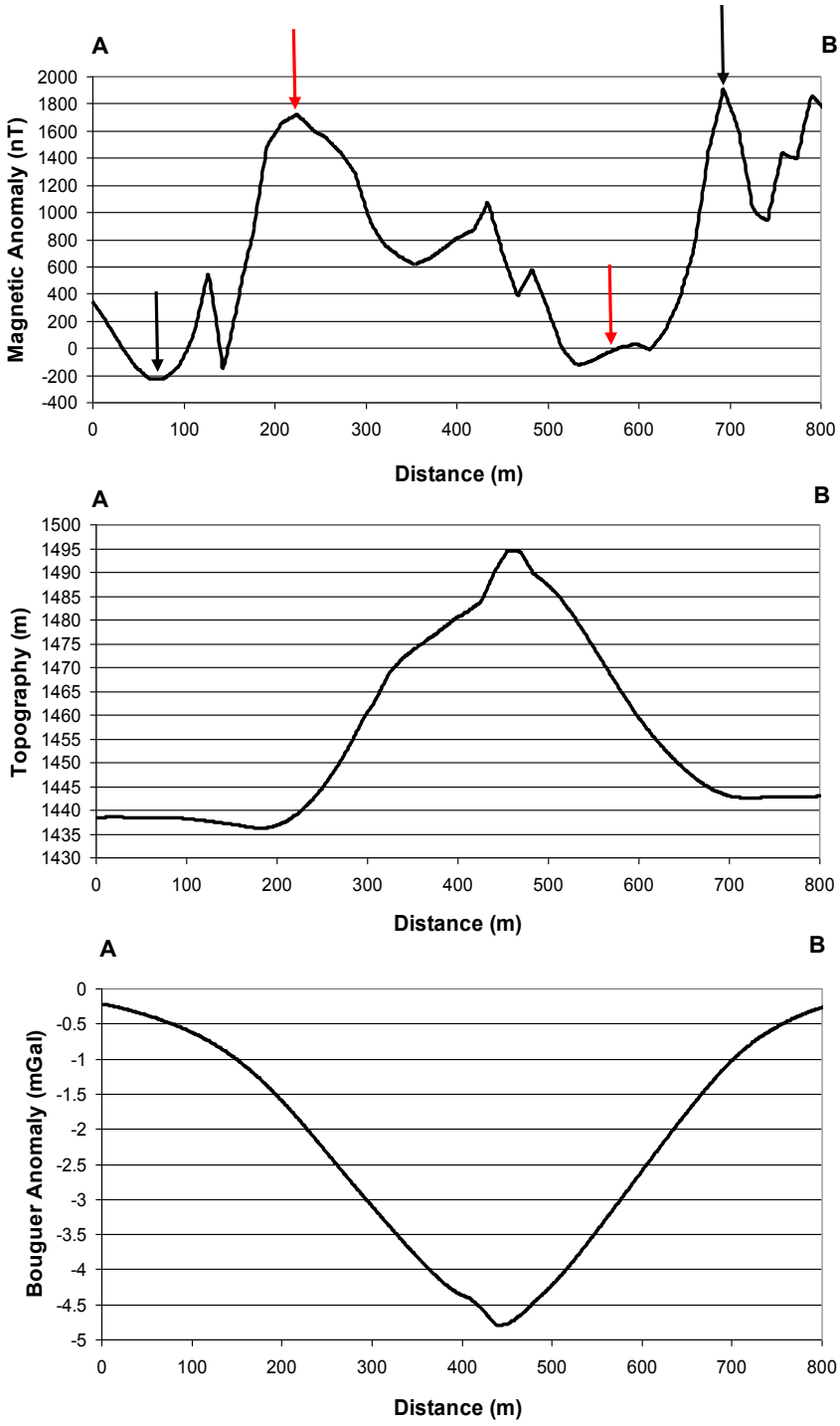

Fig. 11. Top: Magnetic anomaly (nT) detected across Las Bombas volcano and its surrounding "circular pattern" along AB profile (black arrows: indicate minimum and maximum values of the reverse dipolar magnetic anomaly corresponding to the border of the "circular pattern"; red arrows: indicate minimum and maximum values of the normal dipolar magnetic anomaly associated with the scoria cone). Middle: The corresponding topography along AB profile is shown. Bottom: Complete Bouguer Anomaly (mGal) detected across Las Bombas volcano and its surrounding "circular pattern" along AB profile. (For interpretation of the references to colour in this figure legend, the reader is referred to the web version of this article.)

3 m shoulder circular depression, surrounded by the lava flows, are younger than the surrounding lava flows. Similar circular features have been described elsewhere such as "neck in a basin" (NIB) landform that is proposed for volcanic structures characterized by nearly circular to elliptical open basins, located near the headwater of small streams or drainages, which contain small volcanic necks and/or erosion remnants of one (or more) cinder cones (Aranda-Gomez et al., 2010). NIB landforms are typically 400–1000 m in diameter and 30–100 m deep and are invariably surrounded by steep walls cut into one or more basaltic lava flows (Aranda-Gomez

et al., 2010). NIB landforms lack evidence for a primary volcanogenic origin through either collapse or youthful eruptive activity. NIB landforms are erosional features where the central feeder dyke- and neck-dominated part of an older scoria cone that was engulfed by a younger lava flow has been preserved after differential erosion, that removed the outer less welded and more loose portion of the older scoria cone once acted as a barrier for the engulfing younger lava flows (Aranda-Gomez et al., 2010).

In contrast, the *inverse steptoes* identified at LVF such as the LB volcano, are strikingly different from the NIB landforms. First, the central portion of the preserved scoria cones are fairly intact, and there is clear evidence of the presence of still standing volcanic cones and craters. The geological and geophysical evidence also indicates a reverse chronological order; the volcano in the depression is younger than the surrounding flow fields and therefore the feature cannot be a NIB.

The LB volcanic edifice, although partially eroded, is still preserved and its cone flank clearly sits on a circular depression around the cone filled by sand.

The gravity survey indicated a significant negative Bouguer anomaly beneath the scoria cones, suggesting presence of low density material beneath the centre part of the depression that can be interpreted as mass deficit. This can be explained if the lava flow that currently surrounds the scoria cones has been fractured significantly, giving place for a future younger scoria cone to emerge in the newly formed depression. Another possible explanation could be that the roots of the cone have been partially refilled with low-density material. A logical explanation could be that an initial phreatic explosive eruption cut through the older basalt lava flow field that formed an initial depression and later on a scoria cone erupted into that depression. Unfortunately, there is no outcropping pyroclastic succession that would support this interpretation. However, the formation of the depression must be associated with the formation of the volcanic events that formed the basin infilling scoria cones. It is very unlikely that the relationship between the depression and the scoria cone is coincidental.

A possible explanation for this peculiar feature is outlined in Fig. 12.

We can presume that Hawaiian-Strombolian style explosive eruptions occurred with the formation of pyroclastic cones and successive pahoehoe lava flows (Fig. 12-1). During a long period of intense erosion by eolian and minor fluvial processes a significant removal of these cones took place (Fig. 12-2). A new batch of magma was rising, causing the fracturing of the older solidified lava succession (Fig. 12-3). The explosive disruption could have occurred due to a sudden degassing of the rising magma in the near surface, which potentially opened up new fractures and gravitationally destabilised the older solidified lava flows (Fig. 12-4). Perhaps we cannot rule out an initial phreatic explosive event triggered by the explosive interaction between magma and water that was trapped between solidified lava flow units (Fig. 12-5). When the fracturing, decompression and sudden discharge of fractured blocks due to the explosion ended, the magma built a new cone in the newly formed depression on the solidified lava surface (Fig. 12-6). The deposits produced prior to the magmatic eruptions are not preserved in the circular zones around the cone and the old solid flows, perhaps due to extreme arid and windy conditions (Fig. 12-7). A new period of degradation of the cone by climatic forces took place leading to the present day scenario, with a scoria cone of reduced size where cone heights range between 20 and 100 m and slope angles (17–21°) much lower than the ones of young scoria cones expected to have. The modification of the cone geometry (height and width) over time opened a gap between the cone and the old lava flows, allowing it to function as a small sedimentary basin around the cone, collecting eolian as well as sheetwash deposits from the new cone (Fig. 12-8). From the air, these depressions look circular ("circular patterns") and surrounding relatively young scoria cones as it can be seen in (Fig. 5E).

8. Conclusions

The results of the geophysical studies carried out in this work,

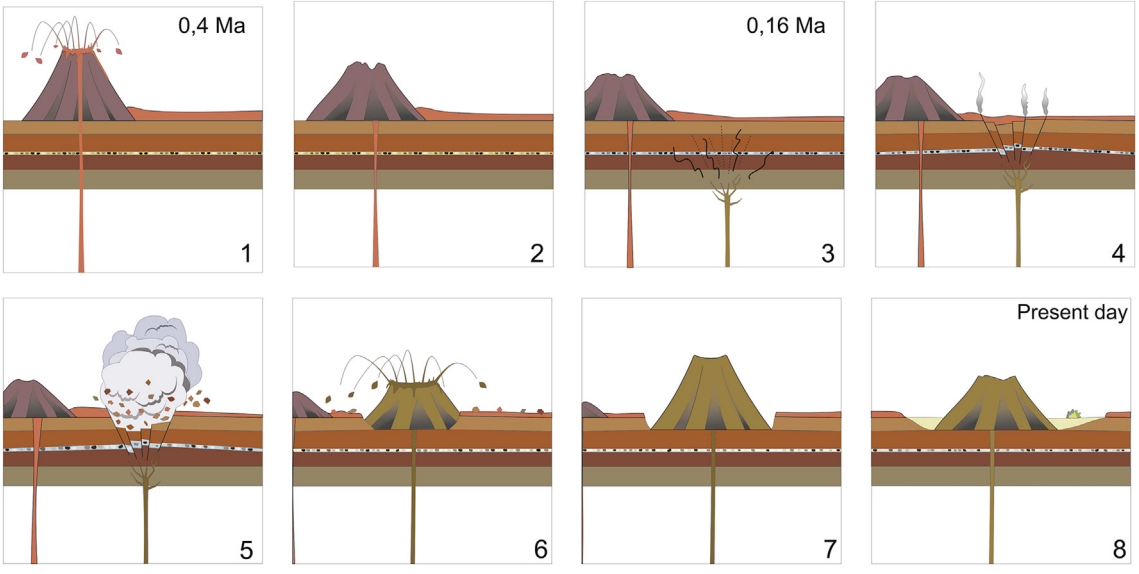

Fig. 12. Geological sketch (out of scale) showing the development of the "circular pattern" during time.1: Hawaiian-Strombolian style eruptions occurred with the formation of pyroclastic cones and successive pahoehoe lava flows. 2: A long period of intense degradation eroded the cones. 3: A new batch of magma caused the fracturation of the older solidified lava succession. 4: The explosive disruption potentially opened up new fractures and gravitationally destabilised the older solidified lava flows. 5: Perhaps an initial phreatomagmatic explosive event triggered the eruption. 6: When the fracturing, decompression and sudden discharge of fractured blocks due to explosion ended, the new magma could built a new cone. 7: A new volcano was born: Las Bombas volcano. 8: A new period of degradation of the cone by climatic forces took place leading to the present day scenario, with a scoria cone of reduced size surrounded by a small sedimentary basin ("Circular pattern") around the cone.

support the model proposed here for the formation of the "circular patterns" that surround the scoria cones located along lineaments in the Llancanelo Volcanic Field, Mendoza, Argentina.

Such "circular patterns" would have been formed by fracturing of the older basaltic lava flows associated with reverse dipolar magnetic anomalies. These older lava flows, due to their reverse polarity and their textural similarities to older lava flows, are assigned to the Chapúa Formation and are inferred to be the same age. The fracturing of these flow sheets were inferred to be caused either by the sudden degassing of a newly intruded younger magma beneath the thick (~40 m) sheet flows, or by a short-lived single phreatic explosion caused by the interaction of the rising magma and water trapped between the older lava sheets.

The scoria cone preserved in depressions in the lava flow fields were inferred to be younger than the flow field as being normal magnetic polarity their flows. The negative complete Bouguer anomalies beneath the scoria cones suggest mass deficit. This anomaly could indicate the presence of fracture zones in the old basaltic lava flows by the rejuvenated magma intrusions or the existence of low density volcanic rocks corresponding to the roots of the scoria cone.

The young scoria cones were subsequently eroded, reducing their cone heights and slope angles to the level slightly emerging above the surrounding lava flow fields. Along the circular features, steep cliffs developed in the pre-cone lava flows where enhanced erosion created a distinct basin-like zone. The identified morphological features of the circular basin-like, scoria cone-filled landforms indicate that to establish a chronological order between events in a lava flow and scoria cone dominated volcanic field is a complex process. In addition, extensive lava flow fields can act as a seal under subsequently intruding magma degassing can provide gas accumulation may trigger sudden decompression and unroofing or could facilitate sudden explosive interaction between rising magma and trapped water tables.

Acknowledgements

Diurnal variation of the geomagnetic field was generously provided by Prof. Dr. Francisco Ruíz from Zonda Magnetic Observatory (San Juan, Argentina). Logistical help by the Dirección de Turismo de Malargüe, and the Dirección de Recursos Naturales Renovables de la Provincia de Mendoza for provided excellent field work conditions. This study was undertaken within the framework of projects granted by ANPCyT (PICT2013-1950) and Buenos Aires University (UBACyT 643/10).

We thank Paul Baldauf (Nova S.U.) for their suggestions and the assistance in the linguistic correction of the manuscript. Journal reviewers, Managing Editor and Technical Editor suggestions greatly improved the quality of this report.

Appendix 1

A number of 451 topographic points were surveyed with a Constructor SP 571145130 Total Station (Fig. 9). The same equipment and methodology has been used in another studies (see: Prezzi et al., 2012; Acevedo et al., 2012). The obtained values were gridded applying the minimum curvature algorithm using the Surface Mapping System software Surfer of Golden Software Inc. This method results in a statistically valid grid of estimated values from unevenly distributed data (e.g. Briggs, 1974; Smith and Wessel, 1990).

Total magnetic field was measured along an approximately N–S profile across LB volcano and the surrounding depression (Fig. 9), using a Geometrics 856 proton precession magnetometer with an equidistance of 10 m between stations. Data obtained were corrected for the diurnal variations in the Earth's magnetic field, and the corresponding IGRF (International Geomagnetic Reference Field) value was subtracted (e.g. Lanza and Meloni, 2006).

Relative gravity measurements were made using a ZLS Burris Standard gravity meter along the same profile (Fig. 9), with an equidistance of 20 m between stations and a precision of 0.01 mGal. The survey was not tied to an absolute gravity station. The geographic location of each measured gravity station was determined with the Constructor SP 571145130 total station. Current standards for reduction of observed gravity to Bouguer anomaly, established by the U.S. Geological Survey (USGS) and the North American Gravity Database Committee, were applied through the use of the spreadsheet for reduction of raw data to the Bouguer anomaly developed by Holom and Oldow (2007). With the additional use of solid earth tide and terrain corrections, the complete Bouguer anomaly was calculated. This spreadsheet (Holom and Oldow, 2007) calculates the corrections for instrument drift, as well as the DC shift (i.e., constant value added or subtracted to observed gravity values) for multiple-day gravity surveys.

To make these corrections, we measured relative gravity in the same base station several times a day during the survey. The average instrument drift correction in each station was of approximately of 0.01 mGal. To calculate height and Bouguer spherical cap corrections, the height above the WGS84 reference ellipsoid for each station was measured using the Constructor SP 571145130 total station with a precision of 0.05 m. Earth tide correction was calculated with the software TSoft version 2.1.15 and entered in the spreadsheet of Holom and Oldow (2007). Finally, terrain correction was performed using as input the topographic grid obtained from the detailed topography survey and also entered in the spreadsheet of Holom and Oldow (2007). The maximum terrain correction was of 0.542 mGal, with an average value of 0.075 mGal.

In the case of paleomagnetic studies, hand samples were collected from the Chapúa Fm. The paleomagnetic samples were oriented using magnetic and solar compasses. A total of 10 hand samples were obtained distributed around the Las Bombas volcano (Fig. 10). Magnetization was measured using a 2G Enterprises cryogenic magnetometer. Detailed alternating fields demagnetization techniques were applied. 18 steps up to fields of 120 mT were performed. Characteristic remanent magnetizations (ChRMs) were isolated using principal components analysis (Kirschvink, 1980) when linear trends of vector end points were identified. The corresponding final-mean direction was determined applying Fisher's (1953) statistics.

References

Acevedo, R., Rabassa, M., Ponce, J., Martínez, O., Orgeira, M., Prezzi, C., Corbella, H., González-Guillot, M., Rocca, M., Subías, I. Y, Vásquez, C., 2012. The Bajada del Diablo astrobleme-strewn field, Argentine Patagonia: extending the exploration to surrounding areas. Geomorphology 169–170, 151–164. http://dx.doi.org/10.1016/j.geomorph.2012.04.020.

Aranda-Gomez, J.J., Luhr, J.F., 1996. Origin of the Joya Honda maar, San Luis Potosi, Mexico. J. Volcanol. Geotherm. Res. 74 (1–2), 1–18.

Aranda-Gomez, J.J., Housh, T.B., Luhr, J.F., Noyola-Medrano, C., Rojas-Beltran, M.A., 2010. Origin and formation of neck in a basin landform: examples from the Camargo volcanic field, Chihuahua (Mexico). J. Volcanol. Geotherm. Res. 197 (1–4), 123–132. http://dx.doi.org/10.1016/j.jvolgeores.2009.08.004.

Bates, R., Jackson, J., 1980. Glossary of Geology, second ed. American Geological Institute.

Bermúdez, A. Y, Delpino, D., 1989. La Provincia Basáltica Andino Cuyana (35–37°L.S. Rev. la Asoc. Geol. Argent. 44, 35–55.

Bermúdez, A., Delpino, D., Frey, F., Saal, A., 1993. Los basaltos de retroarco extraandinos. In: Ramos, V. (Ed.), Geología y Recursos Naturales de Mendoza – 12° Congreso Geológico. Relatorio, pp. 161–172, 1(13).

Bermúdez, A., 1988. Geología y petrología de las formaciones ígneas cenozoicas del Volcán Nevado y áreas adyacentes. UNLP-FCN. Thesis, (Unpublished).

Briggs, I.C., 1974. Machine contouring using minimum curvature. Geophysics 39 (1), 39–48.

Chanell, J.E.T., Hodell, D.A., Curtis, J.H., 2012. ODP Site 1063 (Bermuda Rise)

revisited: oxygen isotopes, excursions and paleointensity in the Brunhes Chron. Geochem. Geophys. Geosystems 13 (2).
Conway, F.M., Ferrill, D.A., Hall, C.M., Morris, A.P., Stamatakos, J.A., Connor, C.B., Halliday, A.N., Condit, C., 1997. Timing of basaltic volcanism along the Mesa Butte fault in the San Francisco volcanic Field, Arizona, from 40Ar/39Ar dates: Implications for longevity of cinder cone alignments. J. Geophys. Res. 102 (B1), 815–824.
Delpino, D., 1987. Erupciones basálticas a través de fracturas en el retroarco andino (35°–36° LS) Mendoza, Argentina. In: International Symposium of Andean Volcanism, vol. IV, pp. 233–237 (San Miguel de Tucumán).
Delpino, D., 1993. Fué el Sur mendocino similar a Hawaii? Evidencias del pasado para entender el presente. In: 1° Jornadas Nacionales de Vulcanología, Medio Ambiente y Defensa Civil. Secretaria de Mineria, Mendoza, pp. 67–77.
Dóniz-Páez, J., Romero, C., Coello, E., Guillén, C., Sánchez, N., García-Cacho, L., García, A., 2008. Morphological and statistical characterisation of recent mafic volcanismo in Tenerife (Canary islands, Spain). J. Volcanol. Geotherm. Res. 173, 185–195. http://dx.doi.org/10.1016/j.jvolgeores.2007.12.046.
Dóniz-Páez, J., Romero-Ruiz, C., Sanchez, N., 2012. Quantitative size classification of scoria cones: the case of Tenerife (Canary Islands, Spain). Phys. Geogr. 33 (6), 514–535. http://dx.doi.org/10.2747/0272-3646.33.6.514.
Easterbrook, D., 2003. In: Quaternary Geology of the United States: INQUA 2003 Field Guide Volume. Geological Society of America, p. 438.
Espanon, V.R., 2010. Cosmogenic ^{21}Ne and ^{3}He Dating and Geochemistry of Young Basaltic Lavas from Southern Mendoza, Argentina. Unpublished Master Thesis, University of Wollongong.
Espanon, V.E., Honda, M., Chivas, A.R., 2014. Cosmogenic ^{3}He and ^{21}Ne surface exposure dating of young basalts from Southern Mendoza, Argentina. Quat. Geochronol. 19, 76–86.
Folguera, A., Naranjo, J.A., Orihashi, Y., Sumino, H., Nagao, K., 2009. Retroarc volcanism in the northern San Rafael Block (34°–35° 30′S), southern Central Andes: occurrence, age, and tectonic setting. J. Volcanol. Geotherm. Res. 186, 169–185.
Fornaciai, A., Favalli, M., Karatson, D., Tarquini, S., Boschi, E., 2012. Morphometry of scoria cones, and their relation to geodynamic setting: a DEM-based analysis. J. Volcanol. Geotherm. Res. 217, 56–72. http://dx.doi.org/10.1016/j.jvolgeores.2011.12.012.
Foshag, W.F., Gonzalez, R.J., 1956. Birth and development of Paricutin volcano, Mexico. U. S. Geol. Surv. Bull. 965-D, 355–489.
Germa, A., Quidelleur, X., Gillot, P.Y., Tchilinguirian, P., 2010. Volcanic evolution of the back-arc Pleistocene Payun Matru volcanic field (Argentina). J. S. Am. Earth Sci. 29, 717–750. http://dx.doi.org/10.1016/j.jsames.2010.01.002.
Gilichinsky, M., Melnikov, D., Melekestsev, I., Zaretskaya, N., Inbar, M., 2010. Morphometric measurements of cinder cones from digital elevation models of Tolbachik volcanic field, central Kamchatka. Can. J. Remote Sens. 36 (4), 287–300. http://dx.doi.org/10.5589/m10-049.
Godchaux, M.M., Bonnichsen, B., Jenks, M.D., 1992. Types of phreatomagmatic volcanoes in the western snake river Plain, Idaho, USA. J. Volcanol. Geotherm. Res. 52 (1–3), 1–25.
González Díaz, E.F., 1972. Descripción Geológica de la Hoja 30d, Payún Matrú, Servicio Nacional Minero Geológico. Bol. (Buenos Aires) 130, 1–92.
Gudnason, J., Holm, P.M., Søager, N., Llambías, E., 2012. Geochronology of the late Pliocene to recent volcanic activity in the Payenia back-arc volcanic province, Mendoza Argentina. J. S. Am. Earth Sci. 37, 191–201.
Gutman, J.T., 2002. Strombolian and effusive activity as precursors to phreato-magmatism: eruptive sequence at maars of the Pinacate volcanic field, Sonora, Mexico. J. Volcanol. Geotherm. Res. 113 (1–2), 345–356.
Hasenaka, T., Carmichael, I., 1985. The cinder cones of Michoacán-Guanajuato, Central Mexico: their age, volume and distribution, and magma discharge rate. J. Volcanol. Geotherm. Res. 25, 105–124.
Heiken, G., 1971. Tuff rings: examples from the fort rock-christmas Lake Valley Basin, south Central Oregon. J. Geophys. Res. 76 (23), 5615–5626.
Hernando, I.R., Llambías, E.J., González, P.D., Sato, K., 2012. Volcanic stratigraphy and evidence of magma mixing in the quaternary Payun Matru volcano, Andean backarc in western Argentina. Andean Geol. 39 (1), 158–179.
Hernando, I.R., Franzese, J.R., Llambías, E., Petrinovic, I.A., 2014. Vent distribution in the quaternary Payún Matrú volcanic Field, western Argentina: Its relation to tectonics and crustal structures. Tectonophysics 622, 122–134.
Holom, D., Oldow, D., 2007. Gravity reduction spreadsheet to calculate the Bouguer anomaly using standardized methods and constants. Geosphere 3 (2), 86–90. http://dx.doi.org/10.1130/GES00060.1.
Inbar, M., Risso, C., 2001. A morphological and morphometric analysis of a high density cinder cone volcanic field – Payún Matru, south-central Andes, Argentina. Z. für Geomorphol. 45, 321–343.
Inbar, M., Gilichinsky, M., Melekestsev, I., Melnikov, D., Zaretskaya, N., 2011. Morphometric and morphological development of Holocene cinder cones: a field and remote sensing study in the Tolbachik volcanic field, Kamchatka. J. Volcanol. Geotherm. Res. 201 (1–4), 301–311. http://dx.doi.org/10.1016/j.jvolgeores.2010.07.013.
Isacks, B., Jordan, T., Allmendinger, R., Ramos, V., 1982. La segmentación tectónica de los Andes Centrales y su relación con la placa de Nazca subductada. Congr. Latinoam. Geol. Actas III, 587–606 (Buenos Aires).
Jaupart, C., Vergniolle, S., 1988. Laboratory models of Hawaiian and Strombolian eruptions. Nature 331, 58–60.
Kay, S., 2002. Magmatic sources, tectonic setting and causes of Tertiary to recent Patagonian plateau magmatism (36°S to 52°S latitude). Actas del XV Congr. Geol. Argent. Calafate. Actas III, 95–100.
Kay, S.M., Burns, W.M., Copeland, P., Mancilla, O., 2006. Upper Cretaceous to Holocene magmatism and evidence for transient Miocene shallowing of the Andean subduction zone under the northern Neuquén Basin. In: Kay, S.M., Ramos, V.A. (Eds.), Evolution of an Andean Margin: a Tectonic and Magmatic View from the Andes to the Neuquén Basin (35°–39° S Latitude). Geological Society of America. Geological Society of America, Colorado, pp. 19–60. Special Paper, 407.
Kereszturi, G., Németh, K., 2012. Monogenetic basaltic volcanoes: genetic classification, growth, geomorphology and degradation. In: Németh, K. (Ed.), Updates in Volcanology – New Advances in Understanding Volcanic Systems. InTech Open, Rijeka, Croatia, ISBN 978-953-51-0915-0, pp. 3–89 doi:10.5772/51387.
Kereszturi, G., Németh, K., Csillag, G., Balogh, K., Kovács, J., 2011. The role of external environmental factors in changing eruption styles of monogenetic volcanoes in a Mio/Pleistocene continental volcanic field in western Hungary. J. Volcanol. Geotherm. Res. 201 (1–4), 227–240. http://dx.doi.org/10.1016/j.jvolgeores.2010.08.018.
Kereszturi, G., Jordan, G., Németh, K., Dóniz-Páez, J.F., 2012. Syn-eruptive morphometric variability of monogenetic scoria cones. Bull. Volcanol. 74, 2171–2185. http://dx.doi.org/10.1007/s00445-012-0658-1.
Kereszturi, G., Geyer, A., Marti, J., Nemeth, K., Doniz-Paez, F.J., 2013. Evaluation of morphometry-based dating of monogenetic volcanoes-a case study from Bandas del Sur, Tenerife (Canary Islands). Bull. Volcanol. 75, 734. http://dx.doi.org/10.1007/s00445-013-0734-1.
Kervyn, M., Ernst, G.G.J., Carracedo, J.C., Jacobs, P., 2012. Geomorphometric variability of "monogenetic" volcanic cones: evidence from Mauna Kea, Lanzarote and experimental cones. Geomorphology 136 (1), 59–75. http://dx.doi.org/10.1016/j.geomorph.2011.04.009.
Lanza, R., Meloni, A., 2006. The Earth's Magnetic Field. Springer, New York, p. 267.
Llambías, E.J., 1966. Geología y petrología del volcán Payún Matrú, Mendoza. Acta Geol. Lilloana, San Miguel Tucumán 7, 265–310.
Llambías, E.J., Bertotto, G., Risso, C., y Hernando, I., 2010. El volcanismo cuaternario en el retroarco de Payenia: una revisión. Rev. la Asoc. Geol. Argent. 67 (2), 278–300.
Martin, U., Németh, K., 2004. Mio/Pliocene phreatomagmatic volcanism in the western Pannonian Basin. In: Geologica Hungarica, Series Geologica, Budapest, vol. 26, p. 198.
Martin, U., Németh, K., 2006. How Strombolian is a "Strombolian" scoria cone? Some irregularities in scoria cone architecture from the Transmexican volcanic Belt, near Volcán Ceboruco, (Mexico) and Al Haruj (Libya). J. Volcanol. Geotherm. Res. 155 (1–2), 104–118. http://dx.doi.org/10.1016/j.jvolgeores.2006.02.012.
Mazzarini, F., D'Orazio, M., 2003. Spatial distribution of cones and satellite-detected lineaments in the Pali Aike volcanic field (southernmost Patagonia): insights into the tectonic setting of a Neogene rift system. J. Volcanol. Geotherm. Res. 125 (3–4), 291–305.
Mazzarini, F., Fornaciai, A., Bistacchi, A. Y, Pasquarè, F., 2008. Fissural volcanism, polygenetic volcanic fields, and crustal thickness in the Payen volcanic complex on the central AndesAndes Foreland (Mendoza, Argentina). G3, 9 (9). http://dx.doi.org/10.1029/2008GC002037.
Morales Volosin, M.S., 2015. Geología del Complejo Volcánico El Pozo, Mendoza-Argentina. Trabajo Final de Licenciatura. FCEN-UBA (Unpublished).
Muñoz, J., Stern, C.R., Bermudez, A., Delpino, D., Dobbs, M.F., Frey, F.A., 1989. El volcanismo Plio-Cuarternario a traves de los 38° y 39° sur de los Andes. Rev. la Asoc. Geol. Argent. 44, 270–286.
Németh, K., 2010. Monogenetic volcanic fields: origin, sedimentary record, and relationship with polygenetic volcanism. In: Cañón-Tapia, E., Szakács, A. (Eds.), What Is a Volcano? GSA Special Papers Volume 470, Geological Society of America, pp. 43–67. GSA Special Papers, 470.
Németh, K., Haller, M., Martin, U., Risso, C., Massaferro, G., 2008. Morphology of lava tumuli from Patagonia (Argentina), mendoza (Argentina) and Al-Haruj (Libya). Z. fur Geomorphol. 52 (2), 181–194. http://dx.doi.org/10.1127/0372-8854/2008/0052-0181.
Ninci, C., 1993. Fotointerpretación geológica del área volcánica sudoriental de Malargüe (Provincia de Mendoza). Gerencia de Exploración Comisión Nacional de Energía Atómica, pp. 1–45. Unpublished Report.
Nullo, F.E., Stephens, G., Combina, A., Dimieri, L., Baldauf, P., y Bouza, P., 2005. Hoja geológica 3569-III/3572-IV Malargüe, Provincia de Mendoza. Servicio Geológico Minero Argentino. Instituto de Geología y Recursos Minerales, Buenos Aires, p. 90. ISSN 0328–2333.
Polanski, J., 1954. Rasgos geomorfológicos del territorio de la provincia de Mendoza: Ministerio Economía, Instituto Investigaciones económicas y tecnológicas. Cuad. Investig. Estud. 4, 4–10.
Prezzi, C., Orgeira, M., Acevedo, R., Ponce, J., Martinez, O., Rabassa, J., Corbella, H., Vásquez, C., González-Guillot, M., y Subías, I., 2012. Geophysical characterization of two circular structures of Bajada del Diablo (Argentina): indication of impact origin. Phys. Earth Planet. Inter. 192–193, 21–34. http://dx.doi.org/10.1016/j.pepi.2011.12.004.
Quidelleur, X., Carlut, J., Tchilinguirian, P., Germa, A., Gillot, P., 2009. Paleomagnetic directions from mid-latitude sites in the southern hemisphere (Argentina): contributions to time averaged field models. Phys. Earth Planet. Inter. 172, 199–209.
Ramos, V.A., Folguera, A., 2011. Payenia volcanic province in the Southern Andes: an appraisal of an exceptional quaternary tectonic setting. J. Volcanol. Geotherm. Res. 201, 53–64.

Ramos, V.A., Kay, S.M., 2006. Overview of the tectonic evolution of southern Central Andes of Mendoza and Neuquén (35°-39°S lat). In: Kay, S.M., Ramos, V.A. (Eds.), Evolution of an Andean Margin: a Tectonic and Magmatic View from the Andes to the Neuquén Basin (35°-39°S Lat). Geological Society of America, Geological Society of America Special Paper, vol. 407, pp. 1–17.

Risso, C., Nemeth, K., Combina, A.M., Nullo, F., Drosina, M., 2008. The role of phreatomagmatism in a Plio-Pleistocene high-density scoria cone field: Llancanelo volcanic field (Mendoza), Argentina. J. Volcanol. Geotherm. Res. 169 (1–2), 61–86. http://dx.doi.org/10.1016/j.volgeores.2007.08.007.

Smith, W.H.F., Wessel, P., 1990. Gridding with continuous curvature Splines in Tension. Geophysics 55 (3), 293–305.

Sumner, J.M., 1998. Formation of clastogenic lava flows during fissure eruption and scoria cone collapse: the 1986 eruption of Izu-Oshima Volcano, eastern Japan. Bull. Volcanol. 60, 195–212.

Valentine, G.A., Gregg, T.K.P., 2008. Continental basaltic volcanoes – processes and problems. J. Volcanol. Geotherm. Res. 177, 857–873. http://dx.doi.org/10.1016/j.jvolgeores.2008.01.050.

Vergniolle, S., Brandeis, G., 1996. Strombolian explosions .1. A large bubble breaking at the surface of a lava column as a source of sound. J. Geophys. Res. Solid Earth 101, 20433–20447.

Vergniolle, S., Manga, M., 2000. Hawaiian and Strombolian Eruptions. In: Sigurdsson, H., Houghton, B.F., McNutt, S.R., Rymer, H., Stix, J. (Eds.), Encyclopedia of Volcanoes. Academic Press, pp. 447–461.

Vergniolle, S., Brandeis, G., Mareschal, J.C., 1996. Strombolian explosions .2. Eruption dynamics determined from acoustic measurements. J. Geophys. Res. Solid Earth 101, 20449–20466.

Vespermann, D., Schmincke, H.-U., 2000. Scoria cones and tuff rings. In: Sigurdsson, H., Houghton, B.F., McNutt, S.R., Rymer, H., Stix, J. (Eds.), Encyclopedia of Volcanoes. Academic Press, pp. 683–694.

Violante, R., Osella, A., de la Vega, M., Rovere, E., Osterrieth, M., 2010. Paleoenvironmental reconstruction in the western lacustrine plain of Llancanelo Lake, Mendoza, Argentina. J. S. Am. Earth Sci. 29, 650–664. http://dx.doi.org/10.1016/j.jsames.2009.12.001.

Walker, G.P.L., 1993. Basaltic-volcano systems. In: Prichard, H.M., Alabaster, T., Harris, N.B.W., Nearly, C.R. (Eds.), Magmatic Processes and Plate Tectonics, Geological Society, London, Special Publications, vol. 76, pp. 3–38.

Yañez, G., Cembrano, J., Pardo, M., Ranero, C., Selles, D., 2002. The challenger- Juan Fernández-Maipo major tectonic transition of the Nazca-Andean subduction system at 33–34° S; geodynamic evidence and implications. J. S. Am. Earth Sci. 15 (1), 23–38.